Completely Multimode Arrayed Waveguide Grating-based Wavelength Demultiplexer

***Abstract*— A multimode fiber-matched arrayed waveguide grating-based demultiplexer has been demonstrated for the first time. In this design, multimode waveguides have been used as array elements. The device, which can be used in short-distance communications, has been realized using low-cost polymer planar waveguide technology. The wavelength channels were succesfully separated. The excess losses of the devices were found to be in the order of 9 dB and the crosstalk was about -7 dB. The performance can be improved significantly by optimizing the design and fabrication technology.**

I. Introduction

THE demand for high bitrates in Local Area Networks (LANs) is increasing rapidly. In order to meet these bitrates, optical data transmission is required. LANs are nowadays built with a combination of optical and electrical data tranmission lines. These optical connection lines allow bitrates of about 600 Mbps. Since LANs are shared by a relatively low number of users, the costs are more important than they are in long-haul networks. To reduce these costs, cheap receivers, transmitters, fibers and components like splitters and switches are necessary. Transmitters that are used in these optical networks, like Vertical Cavity Surface Emitting Lasers (VCSELs), are operating in the wavelength range from 600 to 1000 nm. In this window, a simple Si-detector can be used as a receiver. Multimode fibers are used since they have relaxed alignment tolerances and a less stringent fabrication precision.

A major drawback of multimode technology is modal dispersion, which limits the transmission capacity of the multimode fiber. One of the solutions to increase the capacity to > 1 Gbps is Wavelength Division Multiplexing (WDM). Since the 1990s, multimode fiber-matched WDMs are being developed using diffraction gratings or employing dielectric filters in different configurations [1]. A very cost effective WDM based on an Arrayed Waveguide Grating (AWG) used in the singlemode regime has shown excellent performance [2].

In this article the design, fabrication and characterizations of an AWG-based demultiplexer based on completely multimode waveguides are given. The device is fabricated using very low-cost polymer planar waveguide technology. Polymer planar waveguide technology is a cost effective technology for fabrication of large cross-sectional multimode devices since a wide range of cheap optical polymers is commercially available, thick waveguides can be fabricated easily using very simple equipments and it is suitable for mass fabrication especially when a technique such as molding is used.

In section II the theory of a multimode AWG-based demultiplexer will be treated. In section III the designs of two demultiplexers are described. The fabrication process is given in section IV and in section V the characterization of these two devices is described. Finally, conclusions are given in section VI.

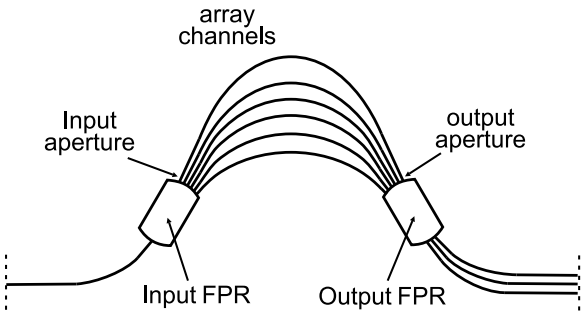

Fig. 1. Layout of the symmetrical Arrayed Waveguide Grating-based Demultiplexer.

II. Theory

A. Principle of operation

In Fig. 1 a schematic representation of an AWG-based demultiplexer is shown. A light beam enters the device at the input channel. After propagation along the input waveguide, the light beam diverges in the input Free Propagation Region (FPR). At the input aperture of the array, the light is coupled into the array channels and propagates along these channels towards the output array aperture.

The array waveguides are chosen such that the path length difference ΔL between each two neighboring waveguides equals an integer multiple m (called the order) of the central wavelength in the array:

$$\Delta L = m\lambda_c / N_{eff,c} \tag{1}$$

where λ_c is the central wavelength in vacuum and $N_{eff,c}$ is the effective refractive index of the array waveguide modes at that wavelength.

At the central wavelength, the fields at the array output aperture of all channels have the same relative phase (apart from an integer multiple of 2π) and intensity distribution. In this way the phase and intensity distribution at the input aperture of the array is reproduced at the output aperture. The light propagating at the central wavelength λ_c coming out of the array converges in the output FPR and is focused into the central output channel in the image plane.

If the wavelength is shifted to $\lambda_c + \Delta\lambda$, there will be a phase change in the individual waveguides that increases linearly from the lower to the upper channel. As a result, the phase front at the output aperture of the array will be slightly tilted, so the beam is focused on a different position in the image

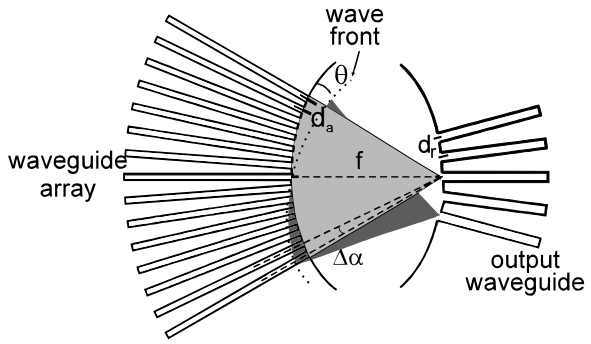

Fig. 2. Layout of the output Free Propagation Region.

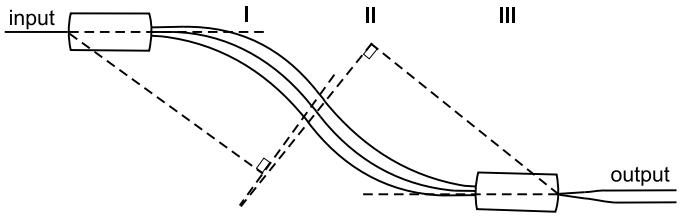

Fig. 3. Layout of a demultiplexer based on an anti-symmetrical or s-bend array geometry.

plane. This is illustrated in Fig. 2. The tilting angle θ_m of the light propagating at a wavelength λ is given by

$$\theta_m \simeq \frac{N_{eff}}{N_f}\frac{\Delta L - m\lambda_g}{d_a} \tag{2}$$

where N_{eff} and N_f are the effective refractive indices in the waveguide array and in the FPRs, respectively, d_a is the pitch between the array waveguides and $\lambda_g = \lambda/N_{eff}$. By placing output waveguides at specific locations in the image plane, a spatial separation of the wavelength channels is achieved [2].

Different geometries can be applied to design an AWG-based demultiplexer [2], [3], [4]. A symmetrical waveguide array, shown in Fig. 1, was first introduced in 1991 by Smit [2] and is now widely used in singlemode optical communication networks. Another array geometry is the anti-symmetrical or s-bend layout, which is shown in Fig. 3. This design was first proposed by Adar et al. in 1993 [4]. In order to properly design and optimize the anti-symmetrical array, it is divided into three sections. Due to the opposite curvatures of sections I and III, the dispersion of the first section is compensated by the last section. Section II accounts for the total dispersion of the array. The path length difference between the waveguides in this part of the array is equal to their total path length difference. The choice for array geometry will be explained in this section.

B. Modal dispersion

The difference in the effective refractive indices in the FPR and in the array waveguides is in our case very small, so $N_{eff}/N_f \simeq 1$. The spectral dispersion D_m is defined as the lateral displacement of the focal spot on the image plane per unit wavelength change. If s denotes the absolute lateral displacement in the image plane and f is the focal length of the array, the dispersion can be expressed as

$$D_m = \frac{ds_m}{d\lambda_g} = f\frac{d\theta_m}{d\lambda_g} = -\frac{N_{eff}}{N_f}\frac{m}{\Delta\alpha} \simeq -\frac{m}{\Delta\alpha} \tag{3}$$

where $\Delta\alpha = d_a/f$ is the divergence angle of the array channels in the array aperture.

Besides dispersion due to the wavelength shift, dispersion also occurs if more than one mode propagates at the same wavelength through the array channels. This so-called modal dispersion can be seen by reviewing Eq. (2), which can be rewritten as

$$\Delta\theta_m = (\frac{\lambda}{N_{eff}} - \frac{\lambda_c}{N_{eff,c}})\frac{m}{d_a} \tag{4}$$

In principle, this formula gives the displacement of the focal spot in the image plane of a certain wavelength λ with respect to the focal spot of the central wavelength. However, the same formula can be used to calculate the worst-case displacement of the focal spot of a certain wavelength due to modal dispersion. As a worst-case estimation, the effective refractive index contrast between different modes propagating at the same wavelength could be taken equal to the refractive index contrast between the core and cladding materials. Then, the displacement of the focal spot of the central wavelength due to modal dispersion can be determined by

$$\Delta\theta_{mod.disp.} = (\frac{\lambda_c}{n_{cladding}} - \frac{\lambda_c}{n_{core}})\frac{m}{d_a} \tag{5}$$

The same formula can be used to calculate the modal dispersion of any wavelength channel. To improve the approximation, the effective indices of the fundamental mode and the highest order mode should be substituted in the expression for $\Delta\theta_{mod.disp.}$. In general, modal dispersion disturbs the exact reproduction of the input field intensity at the image plane, because the focal spot is spread out. In case the array is multimode, the positions of the receiver waveguides should be optimized to keep the losses due to a bad FPR-to-receiver coupling low and to make sure that no light is coupled into an undesired waveguide.

Combining Eqs. (1) and (4) it can be seen that the dispersion increases linearly with increasing path length difference between the array waveguides. This means that if the length difference is kept small, the dispersion will be very small as well, thus broadening the range of wavelengths that are focused on the image plane. The length difference between the array channels can be made much smaller in the anti-symmetrical array geometry than in the symmetrical one. In order to design a broadband AWG-based demultiplexer, the anti-symmetrical array waveguide geometry should be applied.

C. Spectral response

The field in the image plane at the position of the k-th receiver channel is given by [4]

$$E_k(\lambda) = \sum_{j=1}^{n} f_j^2 \exp[ij2\pi N_{eff}(\Delta L + d_a\theta_k)/\lambda] \tag{6}$$

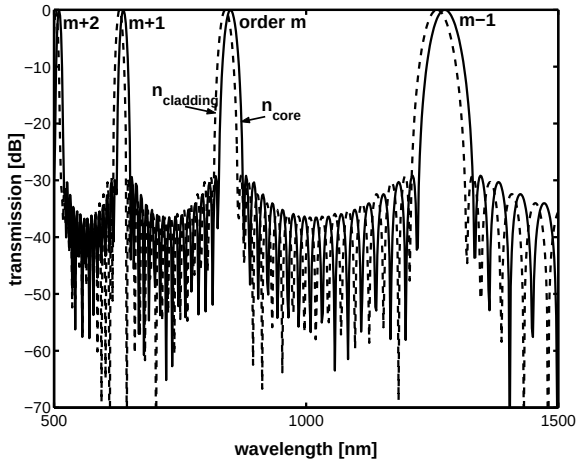

Fig. 4. Spectral response of the lowest and highest order mode at the same wavelength 850 nm of an AWG with $m = 3$ and $n = 17$.

where f_j is determined by the far field of the input and output channels. By good approximation, the field intensity in these channels can be assumed to have a square distribution. From Fourier optics we know that the far field will be a $sinc^2$-function so the coupling coefficient f_j can be expressed as

$$f_j = \frac{\sin^2[\pi/n(j-(n+1)/2)]}{[\pi/n(j-(n+1)/2)]^2} \tag{7}$$

The intensity at the position of the k-th receiver waveguide is given by

$$I_k(\lambda) = |E_k(\lambda)|^2 \tag{8}$$

The spectral response of this receiver waveguide follows as

$$T_k(\lambda) = -10\ \log \frac{I_k(\lambda_k)}{I_k(\lambda)} \tag{9}$$

where the transmission has been normalized so its maximum is 0 dB.

Fig. 4 shows the spectral transmission of one of the receiver waveguides of an AWG of order 3 with 17 array waveguides. The receiver waveguide was designed for a wavelength of 850 nm. In the figure the different orders that are coupled into this output waveguide are shown. With increasing order m (i.e. increasing optical path length difference ΔL), the peaks become narrower and the Free Spectral Range (FSR) decreases.

The FSR can be found by comparing the optical path length difference of orders $m-1$ and m

$$\Delta L = m\frac{\lambda_0}{N_{eff,0}} = (m-1)\ \frac{\lambda_0 + \Delta\lambda_{FSR}}{N_{eff}} \tag{10}$$

Let us define an effective index difference as

$$\Delta N = N_{eff,0} - N_{eff} \tag{11}$$

After some manipulation, the FSR follows from Eq. (10) as

$$\Delta\lambda_{FSR} = \lambda_0 \frac{1 - m\Delta N/N_{eff,0}}{m-1} \tag{12}$$

If we compare the optical path length difference of the m-th order to that of the $(m+1)$-th order, we find the FSR to be

$$\Delta\lambda_{FSR} = \lambda_0 \frac{1 + m\Delta N/N_{eff,0}}{m+1} \tag{13}$$

From Fig. 4, we can intuitively understand that for broadband operation the design of a demultiplexer should be based on an anti-symmetrical AWG. The order of this type of AWG is low, therefore the FSR is large. In case of the AWG of Fig. 4, where the order is 3, the FSR is > 200 nm. This allows for instance for 4 channels with a channel spacing $\Delta\lambda$ of 50 nm. The order of a symmetrical AWG is much larger. If we take for example an order $m = 50$, the FSR will be around 15 nm. This makes the symmetrical AWG not suitable in broadband applications.

In Fig. 4, the transmission of another mode propagating at the same wavelength is also depicted. The two modes for which the transmission spectrum is shown are the highest and lowest order mode, where the effective refractive index contrast is taken to be equal to the contrast between the indices of core and cladding material, as indicated in the figure. In a high-order narrowband AWG, where the spacing $\Delta\lambda$ between the wavelengths is small, broadening due to modal dispersion might cause successive spectral channels to overlap, thus degrading device performance. The lower the order of the AWG, the larger the FSR will be. In that case the spectral channels can still be separated even if the channel spacing is large. In conclusion, a narrowband symmetrical AWG-based demultiplexer can only be made with singlemode array waveguides, whereas the only suitable design for broadband operation with modal dispersion is the anti-symmetrical AWG-based demultiplexer.

III. Design

The fiber-chip losses of the demultiplexer are reduced by adjusting the Numerical Aperture (NA) and the waveguide dimensions of the waveguides to that of the multimode fibers. The NA is defined as

$$NA = \sqrt{n_{core}^2 - n_{cladding}^2} \tag{14}$$

To couple light in and out of the device, $50/125$ μm graded-index multimode fibers with a NA of 0.2 were used. To reduce the fiber-chip losses, the dimensions of input and output waveguides are taken to be 40×40 μm^2. The propagation loss of this waveguide structure are given in section IV. Waveguides with a cross section of 40×40 μm^2 are highly multimodal. The array waveguides are chosen to have dimensions of 15×40 μm^2.

An important building block of the AWG-based demultiplexer are the waveguide bends. Bend losses occur in the array waveguides as well as in the input and output access channels. In bent waveguides, two contributions to bend losses need to be taken in to account [5]. At first, light is lost at the transition from the straight waveguide to the bend due to modal mismatch. The second contribution to bend losses is due to radiation of light as it propagates along the bend of constant radius. It can be described by an attenuation coefficient which

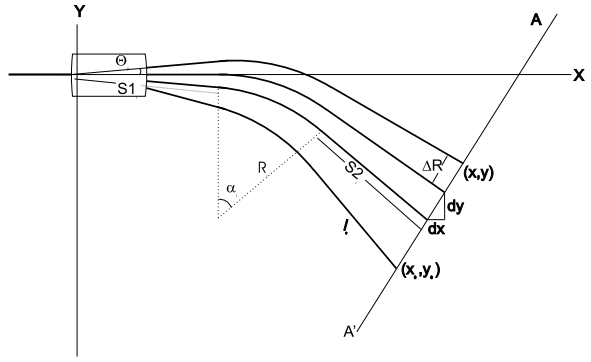

Fig. 5. Details of i-th waveguide of section I of an anti-symmetrical waveguide array.

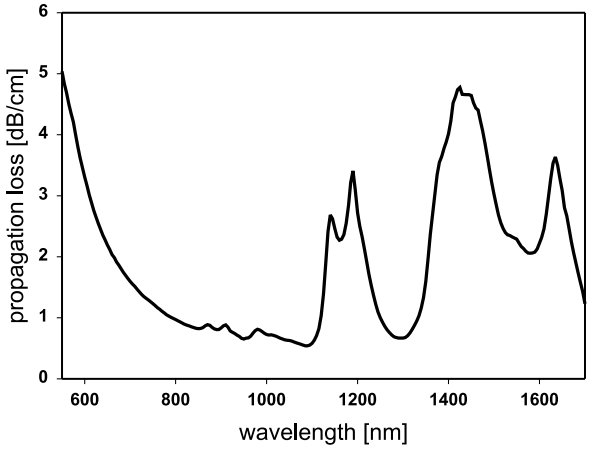

Fig. 6. Propagation loss of a $40 \times 40\ \mu m^2$ SU-8 waveguide.

is independent of the length of the curved waveguide. So far, little research on multimode bends in waveguides has been reported in literature. Israel et al. [6] developed an analytical model for the transmission of a 2D uniform power distribution through a multimode bend. According to the model, which is based on ray optics, the transmission T is given by

$$T = \frac{P_{out}}{P_{in}} = 1 - \frac{1}{2}K - \frac{1}{6}K^2 - \frac{1}{8}K^3 - \frac{1}{8}K^4 + \mathcal{O}(K^5) \quad (15)$$

where

$$K = \frac{n_{core}^2\, w}{NA^2 R} \quad (16)$$

Eq. (15) holds only if $K < 0.5$, which means that the model does not work for bends with very small NA and radius of curvature R. To be on the safe side, all bends in our design are taken to have a radius of curvature > 30 mm.

Two different AWG-based demultiplexers have been designed for central wavelengths 650 and 790 nm. Both designs were made for (de)multiplexing two spectral channels. The effective refractive index in the array waveguides of the demultiplexer with $\lambda_c = 790$ nm was $N_{eff} = 1.5818$ and the spectral channel spacing was 100 nm. The demultiplexer operated at an order $m = 3$ with 16 array waveguides. The pitch between these array waveguide at the start and at the end of the array was 19 μm. The pitch of the two output channels was 55 μm and the free propagation length was 5.576 mm.

Section I of the anti-symmetrical waveguide array is illustrated in Fig. 5. As soon as section I is designed, the design parameters for section III are also determined, since these sections are identical (apart from a rotation). Sections I and III consist of a set of array waveguides that increase linearly in length. Each waveguide is composed of two straight waveguides with a curved part in between and reaches the line A-A' under a normal angle. At the intersection line A-A' the array waveguides are equally spaced.

The length difference ΔL between adjacent array waveguides in this section I can be chosen arbitrarily, but it is an important parameter in the scaling of the device. In the present design it is chosen to be 22.5 μm. The optimum bending angle of the central array waveguide is found to be 22.9 degrees (0.4 radian). The dimensions of the demultiplexer are 46×5.6 mm.

The effective refractive index of the array waveguides at $\lambda_c = 650$ nm was $N_{eff} = 1.5896$ and the spectral channel spacing was 40 nm. The demultiplexer operated at an order $m = 5$ with 18 array waveguides. The pitch between these array waveguide at the start and at the end of the array was 19 μm. The pitch of the two output channels was 55 μm and the free propagation length was 8.363 mm.

As in the former design, the length difference $\Delta L = 22.5$ μm. From the optimization graph the bending angle α_0 is taken to be 25.8 degrees. The dimensions of this demultiplexer are 56×7.5 mm.

IV. Fabrication

The device is made on a borosilicate glass substrate with dimensions of $100 \times 100 \times 1\ mm^3$. The core material SU-8 is a negative photoresist [7]. It is highly transparent for wavelengths > 800 nm, has shown heat resistance to temperatures > 200 degrees Celsius and it is chemically and mechanically stable [8]. The cladding material will be modified lensbond which is a thermal curable adhesive [9].

The SU-8 is spin-coated on the glass substrate. By varying the spin speed, the height of the layer can be varied from 10 to 60 μm. The layer is then pre-baked at 95 degrees Celsius to evaporate the solvent. The film is exposed to UV-light with a mask for 30 seconds. Following the UV-exposure, the film is post-baked at a temperature of 95 degrees Celsius. In this post exposure baking step the cross-linking of the polymer takes place in all exposed areas. The SU-8 film is developed in RER 600 (PGMEA). Finally, the layer is hard-baked at 150 degrees Celsius [8]. The refractive indices of the materials were measured using an Abbe refractometer [10].

The propagation loss spectrum of a straight $40 \times 40\ \mu m^2$ SU-8 waveguide is shown in Fig. 6. The propagation losses of the $15 \times 40\ \mu m^2$ waveguide structure are comparable to that of the former structure.

Measurements on bend losses for bend structures of varying radii of curvature and waveguide width are plotted in Fig. 7 The solid lines are the modeled bend losses of these structures,

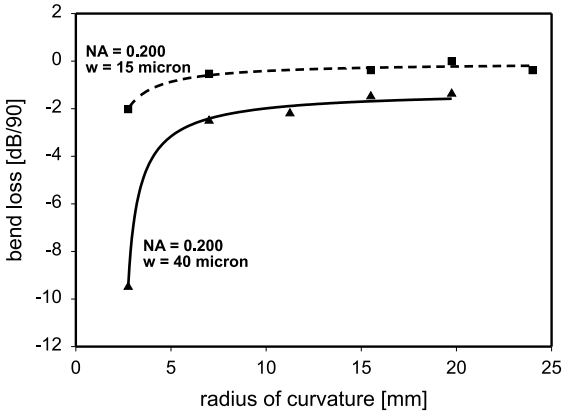

Fig. 7. Bend losses as a function of radius of curvature of three different waveguide structures at a wavelength $\lambda = 850$ nm.

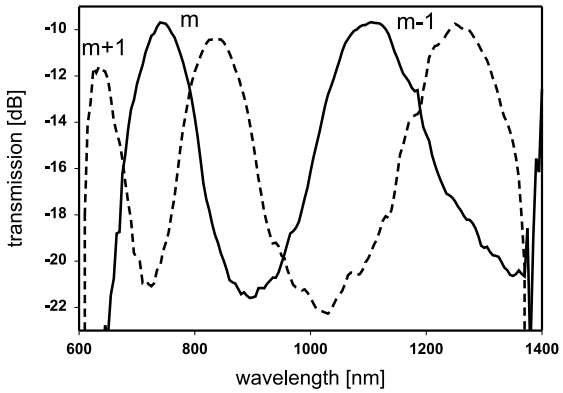

Fig. 8. Measured transmission spectrum of an anti-symmetrical demultiplexer with $\lambda_c = 790$ nm, $\Delta\lambda = 100$ nm (m=3, n=16). The solid line is the transmission of the first receiver waveguide and the dashed line is that of the second one. The spectrum is normalized to that of a straight waveguide.

which are obtained by using Eq. (15). From the figure it can be seen that the critical bend radius for the waveguides with a NA of 0.2 is < 10 mm. Furthermore, it can be seen that bends in 15-μm-wide waveguides exhibit lower bend losses than those in 40-μm-wide waveguides.

V. Results

For measuring the transmission of the fabricated AWG-based demultiplexers, a halogen lamp with a broad spectrum was used as light source. Multimode $50/125$ μm graded-index fibers were used to couple light in and out of the device. Index matching gel was placed in between the chip and the fiber to reduce the fiber-chip losses. The transmission was measured using a spectrometer (Spectro 320 of Instrument Systems) with a resolution of 10 nm.

The spectral response of the first demultiplexer with central wavelength 790 nm is shown in Fig. 8. The spectrum was normalized to that of a straight waveguide. The first receiver waveguide has a peak at 740 nm and the second one has a peak at 840 nm. The excess loss is 10.4 dB with a variation of 0.3 dB. The worst crosstalk level is -10 dB.

For the receiver waveguide centered at 840 nm, the measured FSR at the longer wavelength side is 362 nm and at the shorter wavelength side is 206 nm. The measurement results are in good agreement with the designed FSR, calculated using Eqs. (12) and (13).

In Fig. 9 the transmission spectrum of a demultiplexer that was designed for a central wavelength of 650 nm is shown. The spectrum was normalized to that of a straight waveguide. The peaks in the transmission spectrum are located at $\lambda_1 = 625$ nm and $\lambda_2 = 670$ nm. The excess loss of this demultiplexer was found to be 7 dB with a variation of 0.8 dB. The worst crosstalk level was -6 dB.

Fig. 10 shows a photograph of the output FPR and the receiver waveguides of a demultiplexer. The different orders of the AWG can clearly be seen. It can be seen that a considerable amount of power seems to be radiated into adjacent orders of the same wavelength. Another reason for the high excess losses could be large coupling losses from the FPR to the array due

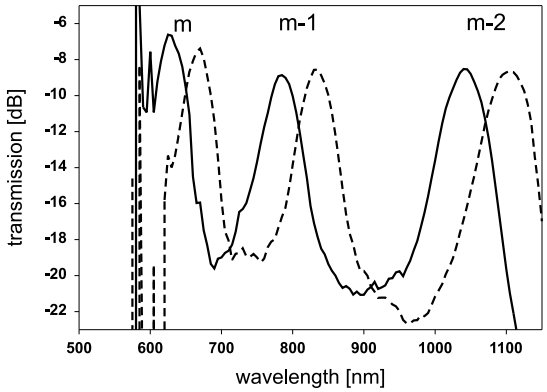

Fig. 9. Measured transmission spectrum of an anti-symmetrical demultiplexer with $\lambda_c = 650$ nm, $\Delta\lambda = 40$ nm (m=5, n=18). The solid line is the transmission of the first receiver waveguide and the dashed line is that of the second one. The spectrum is normalized to that of a straight waveguide.

to a relatively large gap between the array waveguides and a relatively small number of array waveguides.

The high crosstalk values could be caused by irregularities in the opening of the gaps between te array waveguides. Secondly, the modal dispersion causes the peaks to broaden, and therefore power might be coupled into an undesired receiver waveguide.

VI. Conclusion

For the first time, a completely multimode AWG-based demultiplexer has been demonstrated in the wavelength range that is used in LANs. The excess losses of the demultiplexer were found to be 7 to 10 dB and the crosstalk levels were -6 to -10 dB. The device was made using low-cost polymer planar waveguide technology.

The calculated FSR is in good agreement with the measured FSR, which means that the refractive index was measured very accurately using an Abbe refractometer.

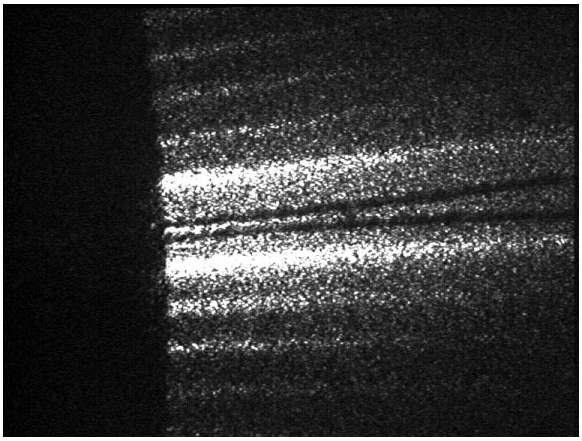

Fig. 10. Photograph of a part of the output FPR and the start of the receiver waveguides of a demultiplexer. The order of highest intensity is coupled into the upper receiver waveguide.

The device is compatible to multimode input and output fibers with a diameter of 50 μm. Fiber-chip losses were reduced to 0.5 dB/facet by adjusting both the dimensions and the NA of the planar waveguides to that of the multimode fibers. The propagation losses of $40 \times 40\ \mu m^2$ SU-8 waveguides are < 1 dB/cm in the region from 800 to 1100 nm and around 1300 nm. At 650 nm, the propagation loss is ~ 2 dB/cm.

Also, bend losses of the used waveguide structure were measured. The bend loss of a 15-μm-wide waveguide with radius of curvature larger than 10 mm is < 0.5 dB/90 and that of a 40-μm-wide waveguide is < 2 dB/90.

REFERENCES

[1] Brian E. Lemoff, Lewis B. Aronson, and Lisa A. Buckman, "SpectraLAN: A Low-Cost Multiwavelength Local Area Network," *Hewlett-Packard Journal*, pp. 42-52, December 1997.

[2] Meint K. Smit, *Integrated Optics in Silicon-based Aluminum Oxide*, PhD thesis, Delft University of Technology, Delft, The Netherlands, 1991.

[3] H. Takahashi, K. Oda, H. Toba, and Y. Inoue, "Transmission Characteristics of Arrayed Waveguide $N \times N$ Wavelength Multiplexer," *J. Lightwave Technol.*, vol. **13**, pp. 447-455, March 1995.

[4] R. Adar, C.H. Henry, C. Dragone R.C. Kistler, and M.A. Milbrodt, "Broad-Band Array Multiplexers Made with Silica Waveguides on Silicon," *J. Lightwave Technol.*, vol. **11**, pp. 212-219, February 1993.

[5] François Ladouceur, and John D. Love, *Silica-based Buried Channel Waveguides and Devices*, Chapman & Hall, London, 1996.

[6] D. Israel, R. Baets, N. Shaw, and M.J. Goodwin, "Study of Multimode Polymeric Waveguide Bends for Backplane Optical Interconnect," *Techn. Digest MOC/GRIN*, 1993.

[7] Microchem, http://www.microchem.com, NANO SU-8 25.

[8] A. Borreman, S. Musa, A.A.M. Kok, M.B.J. Diemeer, and A. Driessen, "Fabrication of Polymeric Multimode Waveguides and Devices in SU-8 Photoresist using Selective Polymerization," *Proc. IEEE/LEOS Symposium (Benelux Chapter)*, The Netherlands, December 2002.

[9] EMSDIASUM, http://www.emsdiasum.com/Summers/optical/cements, Lensbond M-62 with 2.5% plasticizer.

[10] J. Rheims, J. Kose, and T. Wriedt, "Refractive-index measurements in the near-IR using an Abbe refractometer," *Meas. Sci. Techn.*, vol. **8**, pp. 601-605, 1997.